Kinematics of water-bottom and diffracted 2D multiples in data space and image space

Gabriel Alvarez, Stanford University.*

1 SUMMARY

Water-bottom multiples from a dipping interface have the same kinematics in a Common Midpoint (CMP) gather as a primary from a reflector with twice the dip at twice the perpendicular depth at the CMP location. When migrated with the velocity of the primaries, these multiples are over-migrated just as primaries migrated with higher velocity, and their moveout is thus predictable in image space. Diffracted multiples, on the other hand, have an apex-shifted moveout in CMP gathers and a more complicated also apex-shifted residual moveout in image space when migrated with the velocity of the primaries. I illustrate the migration of the multiples with a simple 2D synthetic dataset.

2 INTRODUCTION

Recently, the increased interest in exploration in areas with rough salt bodies, such as the Gulf of Mexico, has sparkled the interest in multiple attenuation methods that work in the image space (Sava and Guitton, 2003; Hargreaves et al., 2004, Alvarez et al., 2004) as opposed to more traditional methods that work in the data space (Hampson, 1986) or Surface Related Multiple Elimination (SRME) (Verschuur et al., 1992; Verschuur et al., 1997) that require dense surface coverage of sources and receivers or demanding data interpolation and extrapolation.

The main advantage of the image space is that most of the complexity of the propagation for the primary reflections is handled by prestack depth migration such that the primary reflections in Angle Domain Common Image Gathers (ADCIG) are flat or nearly flat if the migration is done with the velocity of the primaries. It is not immediately obvious, however, what is the moveout of the migrated multiples. A reasonable approximation is to consider that the residual moveout of the migrated multiples is the same as that of primaries when migrated with the wrong (higher) velocity (Biondi and Symes, 2004). This approach leads, in 2D, to a relatively simple and effective algorithm for the attenuation of the multiples in the image space (Sava and Guitton, 2003) and, with some modifications, can attenuate 2D diffracted multiples reasonably well (Alvarez et al., 2004). In this paper I present the equations for the image space coordinates of the water-bottom multiples in 2D ADCIGs and illustrate the migration of the multiples with a synthetic dataset.

3 KINEMATICS OF 2D MULTIPLES IN DATA SPACE

3.1 Water-bottom multiples

Consider a model with a dipping water-bottom in 2D. The raypath of the primary reflection can be easily computed using the concept of the image source. The moveout of the primary reflection in the CMP domain is given by:

$$t_p = \sqrt{\left(\frac{2Z_D}{V}\right)^2 + \left(\frac{2h_D}{V_{NMO}}\right)^2} = \sqrt{t_0^2 + \left(\frac{2h_D}{V_{NMO}}\right)^2} \quad (1)$$

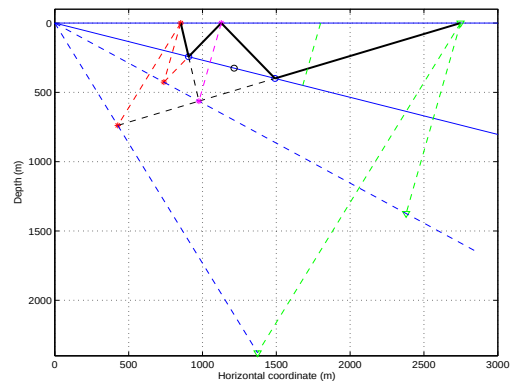

Figure 1. Multiple reflection as a primary from an equivalent reflector with twice the dip angle.

where t_p is the time of the primary, φ is the dip angle of the reflector, Z_D is the perpendicular distance between the surface and the reflector at the CMP location, h_D is half the source-receiver offset, V is the propagation velocity above the dipping reflector, $V_{NMO} = V/\cos\varphi$ is the Normal Moveout velocity and t_0 is the traveltime of the zero-offset reflection.

The raypath of the multiple reflection can be considered as a cascaded of two primary reflections as SRME methods do, but the traveltime of the multiple, t_m, can be computed more easily as the traveltime of an equivalent primary from a reflector dipping at twice the dip angle of the actual reflector as illustrated in Figure 1. That is,

$$t_m = \sqrt{\left(\frac{2\hat{Z}_D}{V}\right)^2 + \left(\frac{2h_D}{\hat{V}_{NMO}}\right)^2} \quad (2)$$

where $\hat{Z}_D$ is the perpendicular distance between the surface and the equivalent reflector with twice the dip at the CMP location and $\hat{V}_{NMO}$ is now $V/\cos(2\varphi)$. Figure 3 shows the primary and the multiple reflection on a CMP gather. Obviously, they are both hyperbolas since the multiple has the same kinematics as a primary.

3.2 Diffracted multiples

Consider now a diffractor sitting on top of the water-bottom reflector at the lateral position x_d and depth z_d. The moveout of the primary diffraction is given by

$$t_d = \frac{\sqrt{(x_d - m_D + h_D)^2 + z_d^2} + \sqrt{(m_D + h_D - x_d)^2 + x_d^2}}{V}$$

where m_D is the horizontal CMP position and h_D is the half-offset between the source and the receiver. This is the equation of a hyperbola with apex at the horizontal position directly above the diffractor. Consider now the multiple that hits the diffractor on its second bounce on the dipping reflector (source-side multiple), as shown in Figure 2. This multiple is no longer the equivalent of any primary, but we can compute its traveltime in the following way:

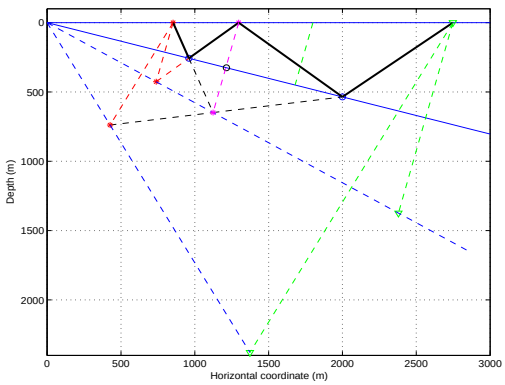

Figure 2. Diffracted multiple. Notice that the last leg of the multiple does not satisfy Snell's law.

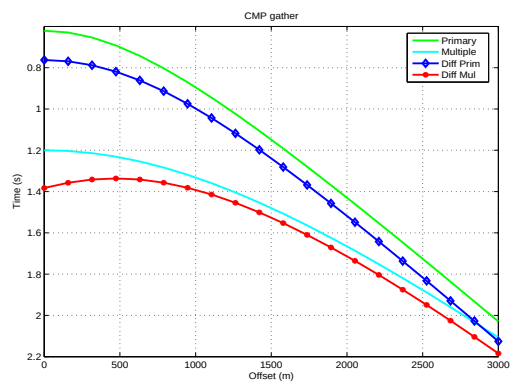

Figure 3. Moveout curves of primary, water-bottom multiple, diffraction and diffracted multiple from a dipping interface on a CMP gather.

(i) Form the image source.

(ii) Find the point at the surface such that the lines joining that point with both the image source and the diffractor intercept with the same angle with respect to the vertical (Snell's law).

(iii) Apply the law of cosines to compute the raypath and divide by the velocity to get the traveltime.

The coordinates of the image source (X_{is}, Z_{is}) are given by

$$X_{is} = X_s - 2Z_0 \sin\varphi \qquad \text{and} \qquad Z_{is} = 2Z_0 \cos\varphi, \quad (3)$$

where $Z_0 = Z_D - h_D \sin\varphi$ is the perpendicular distance between the shot and the reflector.

From the description of numeral 2. above, the coordinate of the multiple bounce at the surface is given by

$$X_{ms} = \frac{X_{is} z_d + x_d Z_{is}}{Z_{is} + z_d}. \quad (4)$$

The aperture angle of the first bounce of the multiple is given by $\beta_s + \varphi$ where β_s is the takeoff angle of the multiple with respect to the vertical. The aperture angle at the surface bounce is $\beta_s + 2\varphi$ and can be easily computed as $\tan(\beta_s + 2\varphi) = \frac{x_d - X_{ms}}{z_d}$. The traveltime of the first leg of the multiple, in terms of β_s and the vertical distance between the source and the reflector $Z_s = \frac{Z_D - h_D \sin\varphi}{\cos\varphi}$ is given by

$$t_{m_1} = \frac{Z_s \cos\varphi}{V \cos(\varphi + \beta_s)}. \quad (5)$$

Similarly, repeated application of the law of sines gives the traveltime of the other three legs of the multiple

$$t_{m_2} = \frac{Z_s \cos\varphi \cos\beta_s}{V \cos(\varphi + \beta_s) \cos(2\varphi + \beta_s)} \quad (6)$$

$$t_{m_3} = \frac{Z_s \cos\varphi \cos\beta_s}{V \cos(2\varphi + \beta_s) \cos(3\varphi + \beta_s)}. \quad (7)$$

The total arrival time of the diffracted multiple is therefore:

$$t_m = t_{m_1} + t_{m_2} + t_{m_3} + \frac{z_d}{V \cos\beta_r} \quad (8)$$

$$= \frac{2(Z_D - h_D \sin\varphi)\cos\varphi}{\cos(\beta_s + 3\varphi)} + \frac{z_d}{V \cos\beta_r}, \quad (9)$$

where $\tan\beta_r = \frac{m_D + h_D - x_d}{z_d}$ and β_r is the emergence angle of the diffracted multiple with respect to the vertical. Figure 3 compares the moveout of the diffracted multiple with that of the water-bottom multiple. Obviously, the apex of the diffracted multiple is not at zero offset.

4 WATER-BOTTOM MULTIPLE IN IMAGE SPACE

The image space coordinates of the water-bottom multiple can be computed by solving the system of equations presented by Fomel and Prucha (1999):

$$t_m = \frac{2\hat{Z}_\xi}{V} \frac{\cos\hat{\varphi}\cos\hat{\gamma}}{\cos^2\hat{\varphi} - \sin^2\hat{\gamma}} \quad (10)$$

$$h_D = \hat{Z}_\xi \frac{\sin\hat{\gamma}\cos\hat{\gamma}}{\cos^2\hat{\varphi} - \sin^2\hat{\gamma}} \quad (11)$$

$$m_D = \hat{m}_\xi + \hat{Z}_\xi \frac{\sin\hat{\varphi}\cos\hat{\varphi}}{\cos^2\hat{\varphi} - \sin^2\hat{\gamma}} \quad (12)$$

where $(\hat{X}_\xi, \hat{m}_\xi, \hat{\gamma})$ are the image space coordinates of the primary kinematically equivalent to the first order water-bottom multiple as mentioned before and $\hat{\varphi} = 2\varphi$. The formal solution of these equations is given by

$$\tan\hat{\gamma} = \frac{2h_D \cos(2\varphi)}{\sqrt{V^2 t_m^2 - 4h_D^2 \cos^2(2\varphi)}} \quad (13)$$

$$\hat{Z}_\xi = \frac{\cos(2\varphi)(V^2 t_m^2 - 4h_D^2)}{2\sqrt{V^2 t_m^2 - 4h_D^2 \cos^2(2\varphi)}} \quad (14)$$

$$\hat{m}_\xi = m_D - \frac{V^2 t_m^2 \sin(2\varphi)}{2\sqrt{V^2 t_m^2 - 4h_D^2 \cos^2(2\varphi)}} \quad (15)$$

These equations allow the computation of the impulse response of the water-bottom multiples in 2D ADCIGs. More importantly, they are the starting point for understanding the kinematics of the data in 3D ADCIGs, still a subject of research.

5 EXAMPLE WITH 2D SYNTHETIC DATA

To illustrate the migration of the multiples, I created a simple 2D synthetic model consisting of a water-bottom reflector dipping at 15 degrees. A diffractor sits on top of this reflector at a horizontal coordinate of 5600 m. The coordinate origin

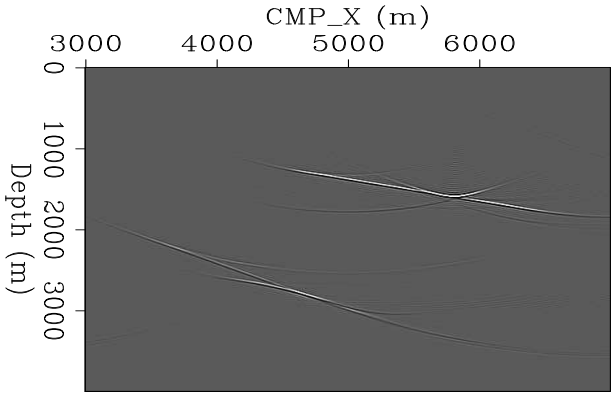

Figure 4. Zero subsurface-offset section extracted from the image obtained by migrating the data with a two constant-velocity layer model. Notice the strong overmigration and poor focusing of the both multiples.

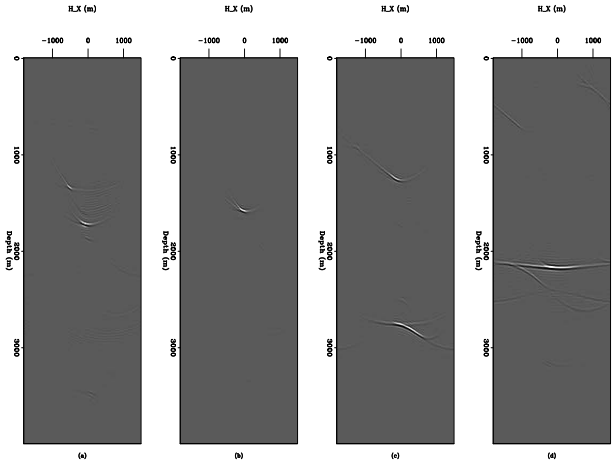

Figure 5. Subsurface-offset common image gathers extracted from the image obtained by migrating the data with a two constant-velocity layer model. (a) at a primary location (CMP_X=6280 m). (b) at the location of the diffractor (CMP_X=5800 m). (c) at a diffracted multiple location (CMP_X=4600 m) and (d) at a water-bottom multiple location (CMP_X=3600 m).

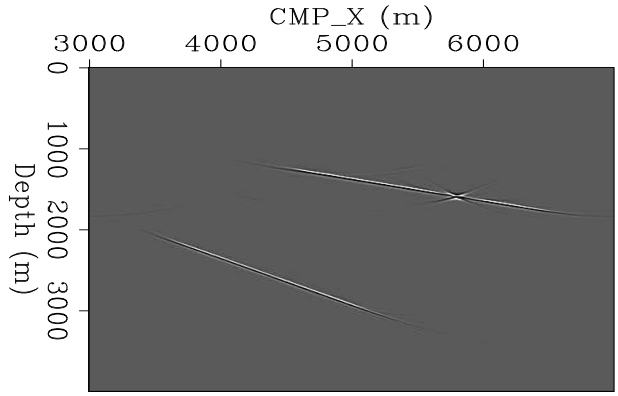

Figure 6. Zero subsurface-offset section extracted from the image obtained by migrating the data with constant water velocity. The water-bottom multiple is properly migrated but the diffracted multiple is not.

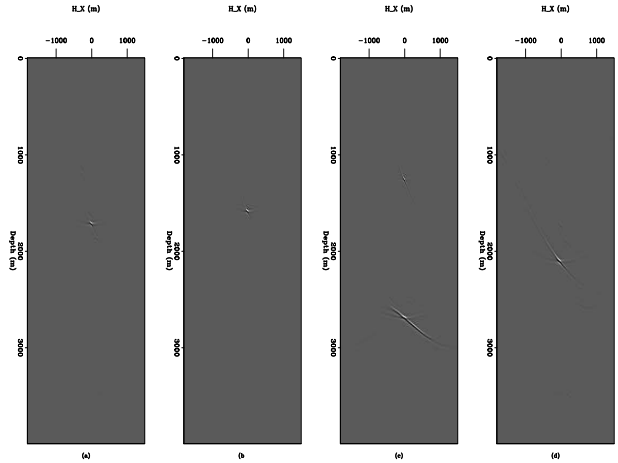

Figure 7. Subsurface-offset common image gathers extracted from the image obtained by migrating the data with constant water velocity. (a) at a primary location (CMP_X=6280 m). (b) at the location of the diffractor (CMP_X=5800 m). (c) at a diffracted multiple location (CMP_X=4600 m) and (d) at a water-bottom multiple location (CMP_X=3600 m).

is the point at which the dipping reflector intercepts the surface. Two hundred CMP gathers were generated with 100 traces in an offset range from 0 to 3000 m. The first CMP corresponds to a horizontal position of 5000 m and the CMP interval is 10 m. I simulated four events: primary, water-bottom multiple, diffraction and diffracted multiple, with a Ricker wavelet with peak frequency of 20 Hz.

Figure 4 shows the zero subsurface offset section extracted from the image obtained by migrating the data with a velocity model consisting of two constant velocity layers: 1500 m/s above the reflector and 2800 m/s below the reflector. I used two reference velocities to migrate the data. As expected, the water-bottom reflector and the diffraction are properly imaged since they were migrated with close to the right velocity. The water-bottom multiple and the diffracted multiple, on the other hand, have both been overmigrated and hence don't look well-focused on this section. This can be seen more clearly in Figure 5 which shows four subsurface-offset common-image gathers extracted from the same migrated image at four different horizontal locations: (a) CMP_X=6280 m corresponding to a primary location; (b) CMP_X=5800 m corresponding to the diffractor location; (c) CMP_X=4600 m corresponding to a diffracted multiple location and (d) CMP_X=3600 m corresponding to a water-bottom multiple location. The primary and the diffractor have their energy concentrated at zero subsurface offset since they were migrated with close to the right velocities. Both multiples, on the other hand, have poor focusing around the zero subsurface offset, since they were migrated with the wrong velocity.

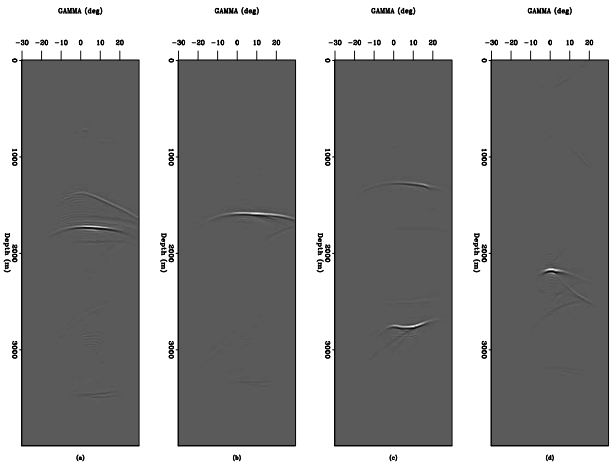

Figure 8. Angle domain common image gathers extracted from the image obtained by migrating the data with a two constant-velocity layer model. (a) at a primary location (CMP_X=6280 m). (b) at the location of the diffractor (CMP_X=5800 m). (c) at a diffracted multiple location (CMP_X=4600 m) and (d) at a water-bottom multiple location (CMP_X=3600 m).

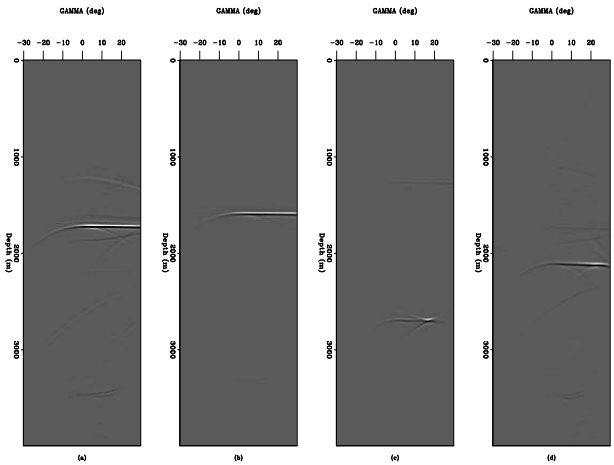

Figure 9. Angle domain common image gathers extracted from the image obtained by migrating the data with constant water velocity. (a) at a primary location (CMP_X=6280 m). (b) at the location of the diffractor (CMP_X=5800 m). (c) at a diffracted multiple location (CMP_X=4600 m) and (d) at a water-bottom multiple location (CMP_X=3600 m).

There is, however, an important difference between the image of the water-bottom multiple and that of the diffracted multiple. This can be seen in Figure 6 that shows the same section as in Figure 4 but extracted from the image obtained by migrating the data with constant water velocity. The primary and the diffractor are perfectly migrated since they were migrated with the exact velocity. The water-bottom multiple is also imaged perfectly as a primary with twice the dip of the real primary. The diffracted multiple, on the other hand, is still poorly imaged and does not show as diffractor at all, since its kinematics do not match those of a primary reflection as explained before. Figure 7 shows the same image gathers as those in Figure 5. Notice the good focusing of the water-bottom multiple.

Since the "natural" prestack domain for velocity analysis of data migrated with wave-equation migration is the aperture angle, it is worth looking at the results of the migration in this domain. Figure 8 shows angle-domain common-image gathers at the same spatial locations as in Figure 5. The primary shows a good coverage of aperture angles. The diffraction samples even more aperture angles, since it is not restricted by Snell's law whereas the water-bottom multiple shows the characteristic overmigration. The diffracted multiple shows as a complicated apex-shifted moveout.

Figure 9 shows the angle-domain common-image gathers extracted at the same spatial locations as in Figure 8 but obtained from the data migrated with constant velocity. Notice how the moveout of the water-bottom multiple is flat like that of the primary but its range of aperture angles is smaller as is intuitively obvious.

6 CONCLUSIONS

I have demonstrated with a simple synthetic dataset that water-bottom multiples from a dipping interface behave as primaries generated by a reflector with twice the dip at twice the perpendicular depth at the CMP location. Therefore they can be perfectly migrated if the migration is done with the water velocity. The diffracted multiples, on the other hand, cannot be perfectly migrated because they do not correspond to an equivalent primary. Understanding how the multiples behave after migration, specially in 3D, is very important for the ultimate goal of attenuating the multiples in image space.

ACKNOWLEDGMENTS

We thank the sponsors of the Stanford Exploration Project for their support to carry out this study.

References

Biondi, B. and Symes, W. 2004, Angle-domain common-image gathers for migration velocity analysis by wavefield-continuation imaging. Soc. of Expl. Geophys., Geophysics, 1283-1298.

Fomel, S., and Prucha, M. 1999, Angle gather time migration. SEP-**100**, 141-150.

Hampson, D. 1986. Inverse velocity stacking for multiple elimination:, *in* 56th Ann. Internat. Mtg. Soc. of Expl. Geophys., Session: S6.7.

Hargreaves, N., and Wombell, R. 2004, Multiple diffractions and coherent noise in marine seismic data: 74th Ann. Internat. Mtg., Soc. of Expl. Geopyhs., 1325-1328.

Sava, P. and Guitton, A. 2003, Multiple attenuation in the image Space. SEP-**113**, 31-44.

Verschuur, D., Berkhout, A. 1997, Estimation of multiple scattering by iterative inversion, part II: practical aspects and examples. Geophysics, **62**. 1596-1611.

Verschuur, D., Berkhout, A., and Wapenaar, C., 1992, Adaptive surface-related multiple elimination: Geophysics, **57**, no. 9, 1166-1167.